ACTA OTORHINOLARYNGOLOGICA ITALICA 2015;35:314-320; doi: 10.14639/0392-100X-693

HEAD AND NECK

Differential diagnosis of parotid gland tumours: which magnetic resonance findings should be taken in account?

Diagnosi differenziale dei tumori parotidei: quali caratteristiche di risonanza magnetica considerare?

T. TARTAGLIONE[1], A. BOTTO[1], M. SCIANDRA[1], S. GAUDINO[1], L. DANIELI[1], C. PARRILLA[2], G. PALUDETTI[2], C. COLOSIMO[1]

[1] Department of Radiological Sciences, Università Cattolica del Sacro Cuore, "A. Gemelli" Hospital, Roma, Italy
[2] Department of Head and Neck Surgery Otorhinolaryngology, Università Cattolica del Sacro Cuore, "A. Gemelli "Hospital, Roma, Italy

SUMMARY

Our aim was to define typical magnetic resonance (MRI) findings in malignant and benign parotid tumours. This study is based on retrospective evaluation of pre-surgical MRI of 94 patients with parotid gland tumours. Histology results were available for all tumours. There were 69 cases of benign (73%) and 25 cases of malignant (27%) tumours, including 44 pleomorphic adenomas, 18 Warthin's tumours, 7 various benign tumours, 6 squamous cell carcinomas, 3 carcinoma ex pleomorphic adenomas, 2 mucoepidermoid carcinomas, 1 adenoid cystic carcinoma and 13 various malignant tumours. The following MRI parameters were evaluated: shape, site, size, margins, signal intensity (SI) on T1w and T2w images, contrast enhancement, signal of cystic content, presence or absence of a capsule, perineural spread, extraglandular growth pattern and cervical adenopathy. Statistical analysis was performed to identify the MRI findings most suggestive of malignancy, and to define the most typical MRI pattern of the most common histologies. Ill-defined margins ($p < 0.001$), adenopathies ($p < 0.001$) and infiltrative grown pattern ($p < 0.001$) were significantly predictive of malignancy. Typical findings of pleomorphic adenoma included hyperintensity on T2w images ($p = 0.02$), strong contrast enhancement ($p < 0.001$) and lobulated shape ($p = 0.04$). Typical findings of Warthin's tumour included hyperintense components on T1w images ($p < 0.001$), location in the parotid inferior process ($p < 0.001$) and mild or incomplete contrast enhancement ($p = 0.01$). SI on T1w and T2w images and contrast enhancement enables differential diagnosis between pleomorphic adenoma and Warthin's tumour.

KEY WORDS: Parotid gland • Neoplasms • Magnetic Resonance Imaging • Differential diagnosis • Histology

RIASSUNTO

La finalità del nostro lavoro è di valutare le caratteristiche di risonanza magnetica (RM) tipiche dei tumori parotidei maligni e benigni. Questo studio retrospettivo si basa sulla valutazione di esami RM pre-chirurgici di 94 pazienti con tumori parotidei. I risultati istologici erano disponibili in tutti i casi; abbiamo analizzato 69 lesioni erano benigne (73%) e 25 maligne (27%): 44 adenomi pleomorfi, 18 tumori di Warthin, 7 tumori benigni di diverso istotipo, 6 carcinomi squamocellulari, 3 carcinomi ex-adenomi pleomorfi, 2 carcinomi mucoepidermoidi, 1 tumore adenoidocistico, 13 tumori maligni di diverso istotipo. Sono state valutate le seguenti caratteristiche RM: morfologia, sede, dimensioni, margini, intensità di segnale nelle sequenze T2-pesate e T1-pesate, impregnazione dopo mezzo di contrasto (mdc), intensità di segnale della porzione cistica, presenza o assenza di una capsula, diffusione perineurale, pattern di crescita extraghiandolare e linfoadenopatie laterocervicali. È stata effettuata un'analisi statistica per identificare le caratteristiche RM più indicative di malignità e per definire l'aspetto tipico degli istotipi più comuni. I parametri significativamente predittivi di malignità sono risultati i margini mal-definiti ($p < 0,001$), le linfoadenopatie ($p < 0,001$) ed il pattern di crescita infiltrativo ($p < 0,001$). Le caratteristiche tipiche dell'adenoma pleomorfo sono risultate l'iperintensità di segnale nelle immagini T2-pesate ($p = 0,02$), l'intensa impregnazione dopo mdc ($p < 0,001$) ed i margini lobulati ($p = 0,04$). Le caratteristiche tipiche del tumore di Warthin sono risultate le componenti iperintense nelle immagini T1-pesate ($p < 0,001$), la localizzazione nel processo parotideo inferiore ($p < 0,001$) e l'impregnazione post-contrastografica lieve/incompleta ($p = 0,01$). L'intensità di segnale nelle immagini T1-pesate e T2-pesate e l'impregnazione post-contrastografica si sono rivelate utili nella diagnosi differenziale tra adenoma pleomorfo e tumore di Warthin.

PAROLE CHIAVE: • *Ghiandola parotide • Neoplasie • Imaging di Risonanza Magnetica • Diagnosi differenziale • Istologia*

Acta Otorhinolaryngol Ital 2015;35:314-320

Introduction

Parotid gland tumours account for approximately 3-6% of all head and neck tumours, with an annual estimated global incidence of 0.4-13.5 per 100,000 persons [1]. About 80% of parotid tumours are benign, the

most common being pleomorphic adenomas [2]. Median age of onset is 45 years, with a peak of incidence for benign tumours in the fourth decade of life; for malignant tumours, the incidence peaks in the sixth or seventh decade [3-5]. Regarding benign tumours, there is a slight overall male preponderance (male:female ratio = 1.1:1), whereas malignant tumours are equally distributed between the two sexes [1].

Most parotid tumours present as slow-growing, painless masses. Symptoms such as local pain, facial nerve palsy, skin ulceration, fast-growing masses, otalgia (related to posterior auricular nerve involvement) and cervical adenopathy should evoke a suspicion of malignancy [6 7].

Because the parotid gland is easily accessible for palpation, it is often possible to characterise the lesion by fine-needle aspiration cytology (FNAC), which has a sensitivity of 0.80 and a specificity of 0.97 [8]. The risk of dissemination of neoplastic cells along the route of the needle is considered negligible [9]. However, FNAC is inconclusive in almost 6% of cases because of insufficient sample size or location of the tumour in the deep parotid lobe [10 11].

Preoperative imaging has assumed a to play major role in surgical planning for assessing tumour location and malignancy. In patients with benign tumours, the surgical procedure may be limited to superficial parotidectomy or extracapsular enucleation, whereas in case of malignant lesions, patients usually undergo total parotidectomy with possible facial nerve sacrifice [12 13]. Ultrasound (US) is accepted as the first imaging method for the assessment of lymph nodes and soft-tissue diseases in the head and neck, including the major salivary glands [14]. However, with US, it is often difficult to study the deep parotid lobe because of the acoustic shadow of the mandible, and it is not possible to visualise the facial nerve, retropharyngeal and deep neck adenopathies and the intracranial or skull base extent of the mass [14-16]. Thus, magnetic resonance imaging (MRI) is considered the most appropriate method for the evaluation of parotid gland tumours owing to its high contrast resolution for soft tissues and capability of visualising deep lobe tumours; it also provides excellent morphological and volumetric assessment, a precise definition of the relationship with adjacent structures and a panoramic view of the cervical lymph nodes [6 15].

Computed tomography has limited use in the assessment of salivary gland tumours and is used only in cases of contraindication of MRI or in claustrophobic patients [17].

The aim of this study was to identify the most useful MRI findings for differential diagnosis of parotid tumours.

Materials and methods

Our study was based on retrospective assessment of pre-surgical and pre-biopsy/pre-FNAC MR examinations obtained in 94 patients (43 females and 51 males; mean age, 43.5 years; range, 15–92 years) with parotid gland tumours and undergoing surgical resection at the Department of Otolaryngology of Catholic University of the Sacred Heart, between February 2005 and September 2014.

In all cases, the MRI protocol included a T1w sequence, a T2w sequence and a T1w sequence with fat saturation after contrast injection. The Ethics Committee approved the study, and all patients provided written, informed consent.

In all patients, surgical specimens were subject to histopathological and immunohistochemical analyses and resulted in 69 benign (73%) and 25 malignant (27%) tumours, including 44 pleomorphic adenomas, 18 Warthin's tumours, 7 various benign tumours (1 haemangioma, 2 myoepitheliomas, 1 ductal cyst, 1 lipoma, 1 oncocytoma, 1 cholesteatoma), 6 squamous cell carcinomas, 3 carcinoma ex pleomorphic adenomas, 2 mucoepidermoid carcinomas, 1 adenoid cystic carcinoma, 13 various malignant tumours (1 sebaceous tumour, 1 myoepithelial carcinoma, 4 undifferentiated tumours, 5 metastases from squamous cell carcinomas of the skin and 2 adenocarcinomas).

Two radiologists with 24 (TT) and 12 (SG) years of experience in head and neck imaging, respectively, examined all pre-surgical MRI results, evaluating the following MRI parameters:

- Site and number of lesions: unilateral or bilateral, single or multifocal. Location in the superficial lobe (subdivided in body, anterior and inferior processes) or deep lobe; an imaginary line drawn from the stylomastoid foramen to the lateral margin of the retromandibular vein was used as a landmark between the deep and superficial lobe.
- Overall morphology: oval, round, lobulated or irregular.
- Dimensions: size along the major axis.
- Margins: well-defined, ill-defined or spiculated; the tumour's margins were evaluated on both pre- and post-contrast T1w images.
- Extraglandular infiltrative growth pattern: invasion of adjacent tissue, including subcutaneous fat, skin, masticatory space or mandible. In patients with multiple lesions with at least one showing infiltrative characteristics, we considered the lesional growth pattern as infiltrative.
- Capsule: a hypointense rim surrounding the lesion on T1w and T2w images, with or without enhancement after contrast injection.
- MRI signal intensity (SI) and enhancement of lesions: on T1w images, lesion enhancement was determined relative to the masseter muscle as hypointense (lower intensity than that of the muscle tissue), isointense (intensity similar to that of the muscle tissue) and hyperintense (higher intensity than that of the muscle tissue); on T2w images enhancement was determined relative to the healthy parotid parenchyma as hypointense, isointense and hyperintense. Enhancement of the tumour was classified as low (less enhancement than

seen for parotid tissue), intermediate (enhancement similar to that of normal parotid tissue) or strong (more enhancement than seen for parotid tissue). Before and after contrast injection, tumour enhancement was divided into homogeneous and heterogeneous lesions. For heterogeneous lesions, the SI and enhancement of the predominant portion of the tumour were evaluated.

- SI of cystic content: based on T1w and T2w images relative to the signal of the lesion and scored as hypointense (lower to that of the lesion), isointense (similar to that of the lesion) and hyperintense (brighter than that of the lesion).
- Perineural spread: pathological enhancing mass along the cranial nerves (V and VII).
- Cervical adenopathy: rounded morphology, short axis > 1 cm, necrosis, lymph node conglomerates, extranodal extension.

In patients with multiple lesions, we included the characteristics of the largest in our analysis.

Each MRI finding for malignant tumours was compared with that for benign tumours by Fisher's exact test (Table 1). An MRI finding with a p value < 0.05 was considered statistically significant. Using the same test, each MRI

Table I. Results of statistical analysis.

Findings	Malignant Tumours (n = 25)		Benign Tumours (n = 69)		p Value, Fisher's Exact Test	PPV¶	NPV¶	Specificity	Sensitivity
	Positive	Negative	Positive	Negative					
Signal Intensity†									
T1-	3	22	9	60	1	0.25	0.73	0.87	0.12
T1+	15	10	35	34	0.4879	0.3	0.77	0.49	0.60
T1=	7	18	25	44	0.6229	0.22	0.71	0.64	0.28
T1*	0	25	13	56	0.0175	0	0.69	0.81	0
T2-	2	23	1	68	0.1716	0.67	0.75	0.99	0.08
T2+	20	5	63	6	0.1544	0.24	0.55	0.09	0.8
T2=	3	22	5	64	0.4346	0.38	0.74	0.93	0.12
CE‡									
0	0	25	3	66	0.5625	0	0.73	0.96	0
1	2	23	7	62	1	0.22	0.73	0.90	0.08
2	5	20	24	45	0.2118	0.17	0.69	0.65	0.2
3	18	7	35	34	0.0987	0.34	0.83	0.49	0.72
Appearance									
Homogeneous	1	24	29	40	< 0.001	0.03	0.63	0.58	0.04
Inhomogeneous	24	1	40	29	< 0.001	0.38	0.97	0.04	0.58
Margins									
Well-defined	3	22	66	3	< 0.001	0.04	0.12	0.88	0.96
Ill-defined or spiculated	22	3	3	66	< 0.001	0.88	0.96	0.96	0.88
Morphology									
Round	1	24	2	67	1	0.33	0.74	0.97	0.04
Oval	11	14	39	30	0.3516	0.22	0.68	0.43	0.44
Lobulated	9	16	28	41	0.8124	0.24	0.72	0.59	0.36
Irregular	4	21	0	69	0.0041	1	0.77	1	0.16
Cists/necrosis	10	15	21	48	0.458	0.32	0.76	0.70	0.40
Sites									
Body	13	12	24	45	0.1557	0.35	0.79	0.65	0.52
Lower extension	2	23	17	52	0.0885	0.11	0.69	0.75	0.08
Anterior extension	1	24	14	55	0.0633	0.07	0.7	0.80	0.04
Parapharyngeal extension	5	20	7	62	0.2919	0.42	0.76	0.90	0.20
More sites									
Superficial lobe	4	21	7	62	0.4752	0.36	0.75	0.90	0.16
Deep lobe	10	15	47	22	0.0020	0.18	0.59	0.32	0.40
Single lesion	15	10	22	47	0.0020	0.41	0.82	0.40	0.32
Multifocal	20	5	65	4	0.0530	0.24	0.44	0.06	0.80
	5	20	4	65	0.0530	0.56	0.76	0.80	0.06
Adenopathy	12	13	1	68	< 0.001	0.92	0.84	0.99	0.48
Perineural spread	1	24	0	69	0.2660	1	0.74	1	0.04
Infiltrative grown pattern	17	8	0	69	< 0.001	1	0.9	1	0.68

† T1- hypointensity with respect to masseter muscle, T1+ hyperintensity with respect to masseter muscle, T1= isointensity with respect to masseter muscle, T1 cysts hyperintense on T1 with respect to lesion, T2- hypointensity with respect to parotid tissue, T2+ hyperintensity with respect to parotid tissue, T2= isointensity with respect to parotid tissue; ‡ 0 = no contrast enhancement, 1: low contrast enhancement, 2: intermediate contrast enhancement, 3: strong contrast enhancement; ¶ PPV: positive predictive value, NPV: negative predictive value.*

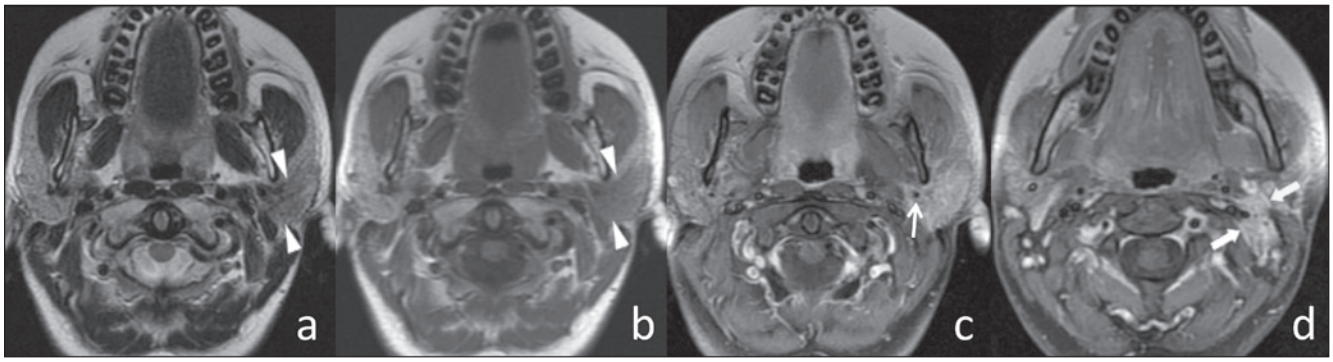

Fig. 1. Squamous carcinoma of the left parotid gland. (**a**) Axial T2w image, (**b**) axial T1w image and (**c** and **d**) axial T1w fat-sat image after contrast injection. The left intraparotid tumour appeared hypointense on T2w and isointense on T1w images (arrowheads) with ill-defined margins. After contrast injection (on T1w fat-sat image), the tumour showed a strong enhancement, encasing the external carotid artery (arrow). Cervical adenopathies were also evident in levels IIa and IIb on the left side (thick arrows).

finding of the most frequent benign tumours (pleomorphic adenomas and Warthin's tumours) was compared with MRI findings from the rest of the benign lesions. The independent samples *t*-test was used for numeric variables such as age and size, whereas the chi-square test was used for gender.

Results

Malignant tumours were more frequent in men (M:F = 2.1:1), whereas benign tumours were equally distributed between the two genders (M:F = 1.02:1); however, a statistical correlation between gender and malignancy was not demonstrated ($p = 0.09$). Among benign lesions, Warthin's tumour was significantly ($p = 0.012$) more common in men (M:F = 4.5:1), whereas pleomorphic adenomas showed the opposite trend (M:F = 1:1.4). The mean age for diagnosis of with malignant tumours was 65.2 years (range, 25–92 years), whereas for benign tumours, it was 50.7 years (range, 15–89 years), with a tendency for malignant lesion to occur in older patients ($p < 0.001$). Patients with pleomorphic adenomas had a lower mean age (44.6 years; range 15–89 years) than patients with Warthin's tumours (60.5 years; range, 47–82 years; $p = 0.012$).

We found multifocal lesions in nine patients: Five cases of metastases from squamous cell carcinomas of the skin, 3 Warthin's tumours and 1 pleomorphic adenoma. In all cases, lesions were unilateral except for the pleomorphic adenoma and one of the Warthin's tumours. Both benign (24 of 69) and malignant (13 of 25) lesions were often located in the body of the parotid gland. In Warthin's tumours, we found a higher frequency of tumour localisation in the inferior process (10 of 18).

Irregular shape was found in 16% (4 of 25) of malignant tumours, whereas none of the benign lesions were characterised by irregular shape ($p = 0.004$; specificity, 1; sensitivity, 0.16). Meanwhile, 100% of the benign tumours and 84% of the malignant tumours showed a round, oval or lobulated shape (Table I). The average size of malignant and benign tumours was 38 and 28 mm, respectively ($p = 0.012$). A total of 88% of malignant tumours and only 0.04% of benign tumours showed ill-defined margins ($p < 0.001$; specificity, 0.96; sensitivity, 0.88; Fig. 1; Table I). Extraglandular infiltrative growth patterns were present in 17 of 25 malignant tumours ($p < 0.001$; specificity, 1; sensitivity, 0.68); none of the benign tumours showed infiltrative grown patterns.

A hypointense capsule surrounding the parotid tumour was more frequent in benign than malignant lesions (56% *vs* 8%), and hence predictive of benignity (VPP 0.95, specificity 0.92, sensitivity 0.57, $p < 0.001$). Hypointense SI on T2w images was highly specific (0.99) of malignancy, but the data was not statistically significant ($p = 0.17$) and showed a low sensitivity (0.08). The majority of malignant (80%) and benign (91.3%) lesions showed high SI on T2w images; hence, the SI on T2w was not useful for differential diagnosis ($p = 0.154$). Also, the inhomogeneous SI seen in lesions was not useful in the differential diagnosis, appearing in 96% of malignant and 58% of benign tumours ($p < 0.001$; specificity, 0.04; sensitivity, 0.58). Contrast enhancement did not significantly correlate with malignancy (Table I). Cystic or necrotic areas did not assist in distinguishing malignant from benign tumours, and were present in 40% of malignant and 30% of benign lesions ($p = 0.458$).

Almost 50% (12 of 25) of malignant tumours showed cervical adenopathies ($p < 0.001$; specificity 0.99; sensitivity 0.48), whereas perineuronal spread occurred in only one malignant lesion ($p = 0.226$; specificity 1 sensitivity, 0.04). An enlarged (short axis, 2.7 cm) cervical lymph node with inhomogeneous SI was found in only one case of benign tumour (Warthin's tumour).

Pleomorphic adenomas and Warthin's tumours were the two most common histologic entities, repre-

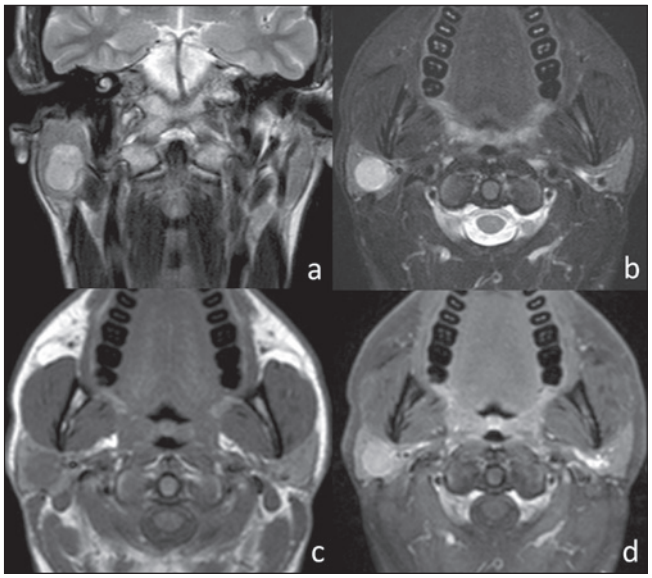

Fig. 2. Pleomorphic adenoma of the right parotid gland. (**a**) Coronal T2w image, (**b**) axial T2w fat-sat image, (**c**) axial T1w image and (**d**) axial T1w fat-sat image after contrast injection. The right intraparotid tumour appeared as an oval lesion, hyperintense on T2w images, and isointense on T1w images, with sharp margins and homogeneous SI. After contrast injection, the lesion showed strong enhancement that was higher than that seen in normal parotid tissue.

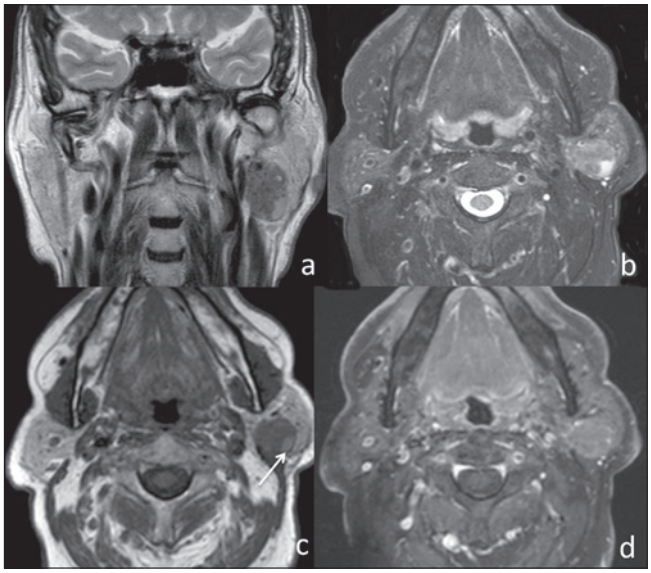

Fig. 3. Warthin's tumour of the left parotid gland. (**a**) Coronal T2w image, (**b**) axial T2w fat-sat image, (**c**) axial T1w image and (**d**) axial T1w fat-sat image after contrast injection. The left intraparotid tumour appeared as an oval lesion with well-defined margins and hypointense on T2w images. T1w images showed a hyperintense cystic area (arrow) within the lesion. After contrast injection, the lesion showed only focal contrast enhancement.

sented by 44 and 18 cases, respectively, accounting for almost 90% of benign parotid tumours. The typical MR findings for pleomorphic adenomas included strong enhancement ($p < 0.001$), high signal on T2w images ($p = 0.02$), oval or lobulated shape ($p = 0.02$ and $p = 0.04$, respectively) and well-defined margins ($p = 0.04$; Fig. 2). For Warthin's tumours, typical MRI findings included cystic areas that were hyperintense on T1w images ($p < 0.001$), low or incomplete contrast enhancement ($p = 0.01$) and location in the inferior process ($p = 0.01$; Fig. 3).

Other histologic entities were present only to a limited extent, yielding non-significant results in statistical analyses.

Discussion

Most studies consistently report that malignant parotid tumours show ill-defined margins, inhomogeneous SI and low SI on T2w images; concomitant cervical adenopathies or perineural spread may be present. Instead, benign tumours are characterised by well-defined margins, a high SI on T2w images and location in the superficial lobe [6 17-19].

Our experience confirmed that the most useful MRI finding in differential diagnosis between benign and malignant lesions was ill-defined margins (before and after intravenous contrast administration, $p < 0.001$; specificity, 0.96; sensitivity, 0.88) [17 18].

However, ill-defined margins are not completely specific of malignancy, but are rarely present in benign tumours with adjacent inflammatory phenomena, as we found in two Warthin's tumours and one haemangioma, leading to possible erroneous diagnostic hypotheses. It has already been reported that this aspect is more frequent in cystadenolymphoma, and inflammatory phenomena could be related to exogenous bacterial contamination or primary infarction of a Warthin's tumour, with subsequent release of intraluminal preformed crystals and inflammation of a foreign body reaction type [20-22].

In contrast, malignant intralesional degeneration is a possible event in lesions with well-defined margins and is common in pleomorphic adenomas, with rates up to 25% [6 17 23].

We encountered three cases of carcinoma ex pleomorphic adenoma with small foci of carcinomatous elements (two adenocarcinoma NOS and one mucoepidermoid carcinoma) that were hardly detectable on MRI and revealed during histological analysis. Pathological cervical adenopathies ($p < 0.001$) and perineural spread ($p = 0.266$) were reliable signs of malignancy, although the p value of perineural spread did not reach statistical significance because it was found in only one case. In one case, we found a Warthin's tumour with adenopathy (inhomogeneous enhancement and a short axis of 2.8 cm) at the V level, which pathologically resulted as a lymph node location of Warthin's tumour. In the literature, there are only few reports on the occurrence of extraglandular Warthin's tumours in cervical lymph nodes, which could

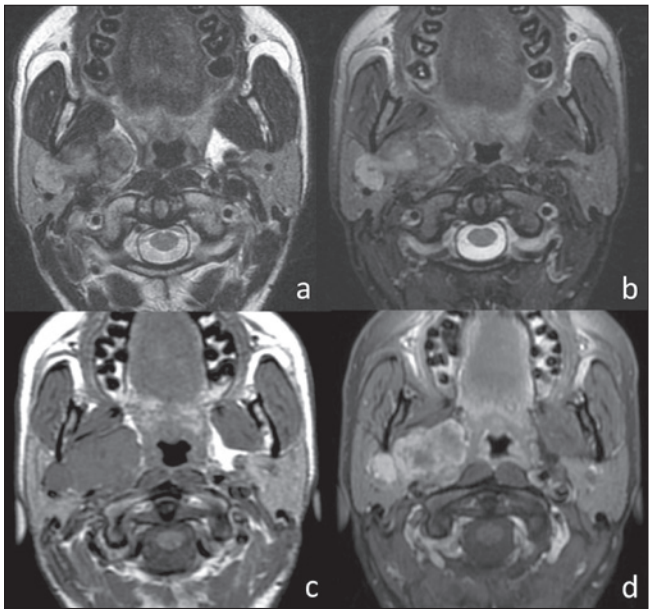

Fig. 4. Atypical pleomorphic adenoma of the right parotid gland. (**a**) Axial T2w image, (**b**) axial T2w fat-sat image, (**c**) axial T1w image and (**d**) axial T1w fat-sat image after contrast injection. The lobulated tumour involved both the superficial and the deep lobe of the right parotid gland, showing sharp margins and inhomogeneous SI on T2w images. After contrast injection, the lesion showed strong inhomogeneous enhancement.

be related to heterotopia of salivary tissue in extra-parotid lymph nodes [24].

Another MRI finding suggestive of malignancy was extraglandular infiltrative growth into surrounding tissue ($p < 0.001$; specificity, 1; sensitivity, 0.68). In fact, it was present only in malignant tumours (68%), whereas none of the benign lesions showed it. Nevertheless, inflammatory lesions could have an infiltrative grown pattern mimicking malignant tumours, and so anamnestic knowledge is essential [19 20]. The dimensions of the lesion also appear to correlate with malignancy (average, 38 mm in malignant lesions *vs* 28 mm in benign lesions, $p = 0.012$).

The SI of solid lesions was less useful in the differential diagnosis between malignant and benign tumours ($p = 0.154$). Contrary to data from other studies, in 80% of malignant and 91.3% of benign tumours the SI on T2-weighted images was higher than in healthy parotid parenchyma. Nevertheless, a hypointense SI on T2w images is highly specific of malignancy (0.99), but in our series, it was present in too few cases to able to demonstrate statistical significance ($p = 0.17$) and with a low sensitivity (0.08) [17 18].

Moreover, the inhomogeneous SI of the lesion was not useful in differential diagnosis, appearing in 96% of malignant and 58% of benign tumours; this MRI finding showed a very low specificity of malignancy (0.04). Furthermore, the SI of benign lesions depends on its dimensions; in fact, we found a higher frequency of inhomogeneous SI in larger lesions, which could be explained by necrotic areas, haemorrhages and cystic degeneration (Fig. 4) [6 17]. In our experience, cysts or haemorrhagic areas within lesions were not useful for differential diagnosis between malignant and benign tumours. However, hyperintense cysts on T1w images in lesions with sharp margins (indicative of benign lesion) appear to be strongly suggestive of Warthin's tumour ($p < 0.001$; specificity, 1.0; sensitivity, 0.72), which has never been found in pleomorphic adenomas, the other most common benign lesion. This finding appears to be related with proteinaceous, haemorrhagic, or cholesterin accumulation [19 25 26].

Contrast injection enabled better definition of lesional margins on T1w fat-saturated images and evaluation of intralesional components (solid *vs* cystic portions), but the degree of tumour enhancement did not enable the distinction between benign and malignant tumours. However, the degree of contrast enhancement differed significantly between pleomorphic adenomas and Warthin's tumours, being strong or complete in the former ($p < 0.001$) and low or incomplete in the latter ($p = 0.01$). These data have already been reported and appear to correlate with the scarce interstitial spaces in Warthin's tumours [18 27 28].

The site of the lesion was not a predictor of malignancy. In fact, the body of the parotid gland was the most frequent site in both malignant and benign tumours. As previously reported, the inferior process of the parotid gland was the most common site of onset of Warthin's tumour (55%, $p = 0.01$) [17].

One limitation of our study was that DWI and perfusion sequences were not routinely performed or considered. These new imaging techniques could add additional information to better characterise parotid lesions [29-32]. Moreover, we mainly observed benign lesions, particularly pleomorphic adenomas ($N = 44$) and Warthin's tumours ($N = 18$), whereas malignant tumours were few and histologically heterogeneous; consequently it was not possible to identify typical MRI findings for each malignant pathological entity.

Conclusions

MRI should be considered the most appropriate imaging modality for parotid gland tumours. In our experience, careful evaluation of lesion margins, SI of cystic content, extraglandular infiltrative growth pattern, cervical lymph nodes and eventual perineural spread may lead to a correct differentiation between malignant and benign parotid lesions. In particular, ill-defined margins are highly predictive of malignancy. Meanwhile, well-defined margins or a hypointense capsule are characteristic of benign lesions.

References

[1] Tian Z, Li L, Wang L, et al. *Salivary gland neoplasms in oral and maxillofacial regions: a 23-year retrospective study of 6982 cases in an eastern Chinese population*. Int J Oral Maxillofac Surg 2010;39:235-42.

[2] Nagler RM, Laufer D. *Tumors of the major and minor salivary glands: review of 25 years of experience*. Anticancer Res 1997;17:701-7.

[3] Eveson JW, Cawson RA. *Salivary gland tumours. A review of 2410 cases with particular reference to histological types, site, age and sex distribution*. J Pathol 1985;146:51-8.

[4] Takahama Junior A, de Almeida OP, Kowalski LP. *Parotid neoplasms: analysis of 600 patients attended at a single institution*. Braz J Otorhinolaryngol 2009;75:497-501.

[5] Aparecida de Oliveira F, Barroso Duarte EC, Teixeira Taveira C, et al. *Salivary gland tumor: a review of 599 cases in a brazilian population*. Head Neck Pathol 2009;3:271-5.

[6] Lee YY, Wong KT, King AD, et al. *Imaging of salivary gland tumors*. Eur J Radiol 2008;66:419-36.

[7] Guzzo M, Locati LD, Prott FJ, et al. *Major and minor salivary gland tumors*. Crit Rev Oncol Hematol 2010;74:134-48.

[8] Schmidt RL, Hall BJ, Wilson AR, et al. *A systematic review and meta-analysis of the diagnostic accuracy of fine-needle aspiration cytology for parotid gland lesions*. Am J Clin Pathol 2011;136:45-59.

[9] Gal R. *Fine needle aspiration of the salivary glands: a review*. Oper Tech Otolaryngol Head Neck Surg 1996;7:323-6.

[10] Yabuuchi H, Fukuya T, Tajima T, et al. *Salivary gland tumors: diagnostic value of gadolinium-enhanced dynamic MR imaging with histopathologic correlation*. Radiology 2003;226:345-54.

[11] Colella G, Cannavale R, Flamminio F, et al. *Fine-needle aspiration citology of salivary gland lesions: a sistematic review*. J Oral Maxillofac Surg 2010;68:2146-53.

[12] Tweedie DJ, Jacob A. *Surgery of the parotid gland: evolution of techniques, nomenclature and a revised classification system*. Clin Otolaryngol 2009;34:303-8.

[13] Chulam TC, Noronha Francisco AL, Goncalves Filho J, et al. *Warthin's tumour of the parotid gland: our experience*. Acta Otorhinolaryngol Ital 2013;33:393-7.

[14] Bialek EJ, Jakubowski W, Zajkowski P, et al. *US of the major salivary glands: anatomy and spatial relationships, pathologic conditions, and pitfalls*. Radiographics 2006;26:745-63.

[15] Yousem DM, Kraut MA, Chalian AA. *Major salivary gland imaging*. Radiology 2000;216:19-29.

[16] Luczewski L, Golusinski P, Pazdrowski J, et al. *The ultrasound examination in assessment of parotid gland tumours: the novel graphic diagram*. Eur Arch Otorhinolaryngol 2013;270:2129–33.

[17] Som M, Curtin HD. *Head and Neck Imaging*. 5th ed. Mosby Inc.; 2011. p. 2449-609.

[18] Christe A, Waldherr C, Hallett R, et al. *MR imaging of parotid tumors: typical lesion characteristics in MR imaging improve discrimination between benign and malignant disease*. Am J Neuroradiol 2011;32:1202–7.

[19] Kinoshita T, Ishii K, Naganuma H, et al. *MR imaging findings of parotid tumors with pathologic diagnostic clues A pictorial essay*. Clin Imaging 2004;28:93-101.

[20] Mantsopoulos K, Psychogios G, Agaimy A, et al. *Inflamed benign tumours of the parotid gland: Diagnostic pitfalls from a potentially misleading entity*. Head Neck 2015;37:23-9.

[21] Patey DH, Thackray AC. *Infected adenolymphoma: a new parotid syndromer*. J Surg 1970;57:569-72.

[22] Rossle M, Winter W, Ihrler S. *A rare cause of subacute parotitis. The pathogenetic role of crystals from an infarcted Whartin's tumour?* HNO 2005;53:969-72.

[23] Motoori K, Yamamoto S, Ueda T, et al. *Inter- and intratumoral variability in magnetic resonance imaging of pleomorphic adenoma*. J Comput Assist Tomogr 2004;28:233-46.

[24] Naujoks C, Sproll C, Deep Singh D, et al. *Bilateral multifocal Warthin's tumors in upper neck lymph nodes. report of a case and brief review of the literature*. Head Face Med 2012;3:8-11.

[25] Ikeda M, Motoori K, Hanazawa T, et al. *Warthin tumor of the parotid gland: diagnostic value of MR imaging with histopathologic correlation*. Am J Neuroradiol 2004;25:1256-62.

[26] Kato H, Kanematsu M, Watanabe H, et al. *Salivary gland tumors of the parotid gland: CT and MR imaging findings with emphasis on intratumoral cystic components*. Neuroradiology 2014;56:789-95.

[27] Suenaga S, Indo H, Noikura T. *Diagnostic value of dynamic magnetic resonance imaging for salivary gland diseases: a preliminary study*. Dentomaxillofac Radiol 2001;30:314-8.

[28] Hisatomi M, Asaumi J, Yanagi Y, et al. *Diagnostic value of dynamic contrast-enhanced MRI in the salivary gland tumors*. Oral Oncol 2007;43:940-7.

[29] Eida S, Sumi M, Nakamura T. *Multiparametric magnetic resonance imaging for the differentiation between benign and malignant salivary gland tumors*. J Magn Reson Imaging 2010;31:673-9.

[30] Espinoza S, Halimi P. *Interpretation pearls for MR imaging of parotid gland tumor*. Eur Ann Otorhinolaryngol Head Neck Dis 2013;130:30-5.

[31] Celebi I, Mahmutoglu AS, Ucgul A, et al. *Quantitative diffusion-weighted magnetic resonance imaging in the evaluation of parotid gland masses: a study with histopathological correlation*. Clin Imaging 2013;37:232-8.

[32] Yabuuchi H, Matsuo Y, Kamitani T, et al. *Parotid gland tumors: can addition of diffusion-weighted MR imaging to dynamic contrast enhanced MR imaging improve diagnostic accuracy in characterization?* Radiology 2008;249:909-16.

Received: April 23, 2015 - Accepted: May 6, 2015

Address for correspondence: Tommaso Tartaglione, Department of Radiological Sciences, Università Cattolica del Sacro Cuore, "A. Gemelli" Hospital, largo A. Gemelli 8, 00168 Rome, Italy. Tel. +39 06 30156054. Fax +39 06 35501928. E-mail: tommaso.tartaglione@gmail.com